# Polyurethanes from Benzene Polyols Synthesized from Vegetable Oils: Dependence of Physical Properties on Structure

**Marie-Josée Dumont,[1] Xiaohua Kong,[1] Suresh S. Narine[2]**

[1]*Alberta Lipid Utilization Program, Department of Agricultural Food and Nutritional Science, 4-10 Agriculture/Forestry Center, University of Alberta, Edmonton, Alberta, Canada T6G 2P5*
[2]*Trent Biomaterials Research Program, Department of Physics, Astronomy and Chemistry, Trent University, Peterborough, Ontario, K9J 7B8*

Received 14 May 2009; accepted 30 January 2010
DOI 10.1002/app.32224
Published online 3 May 2010 in Wiley InterScience (www.interscience.wiley.com).

**ABSTRACT:** Asymmetric and symmetric aromatic triol isomers were synthesized from erucic acid. The pure asymmetric and symmetric triols were crosslinked with MDI into their corresponding polyurethane sheets. The physico-chemical properties of these polyurethanes were studied by Fourier transform infrared (FTIR) spectroscopy, X-ray diffraction (XRD), differential scanning calorimetry (DSC), dynamic mechanical analysis (DMA), thermogravimetric analysis coupled with Fourier transform infrared (TGA-FTIR) spectroscopy, and tensile analysis. The A-PU and S-PU demonstrated differences in their glass transition temperatures ($T_g$) and crosslinking densities. The difference in $T_g$ of these polyurethanes could be explained by the differences in crosslinking densities, which could be related to the increase in steric hindrance, to the crosslinking MDI molecules, between adjacent hydroxyl groups of the asymmetric triol monomers. Overall, it was found that both polyurethanes had similar mechanical and thermal properties. © 2010 Wiley Periodicals, Inc. J Appl Polym Sci 117: 3196–3203, 2010

**Key words:** networks; polyurethanes; renewable resources

## INTRODUCTION

The search for suitable mechanical and physical properties of vegetable oil based polyurethanes (PUs) has generated several academic publications and patents which were recently reviewed.[1] One of the approaches to improved properties is to modify the chemical structure of the polyols, either by the addition of reactive groups (functionality), modifying the placement of the functional groups on the polyol molecule, or modifying the structure of the polyol molecule. The literature details several chemical reactions performed on different types of vegetable oils that seeks to serve this purpose.[2–19] Generally, these efforts have led to the formation of aliphatic polyols having their hydroxyl groups in secondary[3,6–8,18,19] and primary positions.[4,5,10,14,20]

Recently, Lligadas et al.[21] and Yue and Narine[22] synthesized aromatic polyols with a functionality of 3 from erucic and oleic acid, thereby introducing another class of vegetable oil derived polyols for research into the effect on physical properties. These monomers are different from the aromatic monomers synthesized by Suresh and Kishanprasad,[23] who also developed an aromatic triol from cardanol but where not all of the alcohol groups were located on terminal primary position. Shortly after the work of Lligadas et al.[21] and Yue and Narine,[22] Song and Narine[24] synthesized an aromatic hexaol from oleic acid. Although this publication focuses on the triols produced by Yue and Narine,[22] work continues in the Trent Biomaterials Research Program to examine the effects of the structure of the hexaols on polyurethane properties.

The chemical route to the synthesis of the aromatic triols produced a mixture of asymmetric and symmetric triols isomers, which have their terminal hydroxyl groups in position 1, 3, 4 and 1, 3, 5, respectively. The presence of the phenyl ring within the polyol structure is of interest due to the potential to increase the rigidity of resulting polyurethane sheets, which was normally achieved through addition of an aromatic isocyanate. Yue and Narine[22] focused their efforts on the synthesis and separation of the symmetric and asymmetric triols, while Lligadas et al.[21] synthesized the aromatic triols and polymerized the mixture (M-PU) without further separation of the isomers. The M-PU matrices where synthesized with 4,4′-methylenebis(phenyl isocyanate) (MDI) and different ratios of chain extenders. The objective of this present study was to

*Correspondence to:* S. S. Narine (sureshnarine@trentu.ca).
Contract grant sponsors: NSERC, Bunge Oil, the Alberta Crop Industry Development Fund, the Alberta Canola Producers Commission, the Alberta Agricultural Research Institute.

polymerize the asymmetric and symmetric triols separately with MDI and to understand the effect of the hydroxyl positioning on the different physical and mechanical properties of the PU matrices. This study also compared the properties of the A-PU and S-PU matrices with the properties found for the M-PU matrix containing no chain extenders unless specified in the text. It also provided additional physical and mechanical information that can be extended to the M-PU matrix.

## MATERIALS AND METHODS

### Material

Bromine (99.8%) was purchased from ACROS Organics (Geel, Belgium), and hydrochloric acid was purchased from Caledon (Georgetown, Ontario, Canada). The following reagents were purchased from Fisher Scientific, (Canada): diethyl ether anhydrous (ACS grade), sodium thiosulfate anhydrous (certified), hexane (ACS grade), ethyl acetate (ACS grade), sodium sulfate (10–60 mesh, ACS), 1-propanol (certified), potassium hydroxide (ACS), heptane (HPLC grade), and isopropanol (HPLC grade). The following reagents were purchased from Sigma-Aldrich Co.: erucic acid (90%), dimethyl sulfoxide (>99.5%), tetrahydrofuran (>99.9%), lithium aluminum hydride reagent grade (95%), palladium 10 wt % (dry basis) on activated carbon (wet), and chloromethylsilane redistilled (99%). The Bayer Corporation (Pittsburg) donated the aromatic diphenylmethane diisocyanate (MDI, Mondur MRS) having a functionality of 2.6 and a NCO content of 31.5 wt %.

### Synthesis, separation, and characterization of isomeric triols

The asymmetric and symmetric triol monomer synthesis procedure and characterization by $^{1}H$ NMR and $^{13}C$ NMR were described elsewhere.[22] The hexa-substituted benzene derivatives containing three alcohols groups were synthesized from erucic acid derivatives followed by a cyclotrimerization step catalyzed by palladium on activated carbon and chlorotrimethylsilane (TMSCl), such has described by Yue and Narine.[22] Both types of triols had a functionality of 3 and an equivalent weight of 323 g/mol. A combiflash companion/TS/SMM apparatus from Teledyne ISCO was used for the separation of the triol isomers. The separation of the isomers was verified with a HPLC model 1200 series from Agilent equipped with an ELSD 2000 detector from Alltech. The polar column used for the separation was a diol 100 from Thermo. The solvent system was a mixture of isopropanol and heptane in a molar concentration of 1 : 1 used in a gradient of 0–30%, while 100% heptane was used in a gradient of 100–70%. The flow rate used was of 1 mL/min. The HPLC spectra did not show the presence of impurities for both triols.

### Preparation of polyurethanes

Polyurethane sheets were prepared with the asymmetric triols and symmetric triols and were polymerized with MDI with an OH : NCO ratio of 1 : 1.02. The MDI equivalent weight (EW) was provided by the supplier (133 g/mol). The OH : NCO ratio mentioned above was calculated using the following equation[25]:

$$\text{Molar Ratio} = \frac{\text{Weight Polyol}/\text{Equivalent Weight Polyol}}{(\text{Weight PU} - \text{Weight Polyol})/\text{Equivalent Weight Isocyanate}} \quad (1)$$

The plastic sheets were prepared by homogenously mixing MDI with the corresponding triols. The mixtures were then cast into a plastic mold and cured at 75°C for 24 h.

### FTIR

The FTIR equipment used was a Nicolet Magna 750 coupled with a MCT-A detector and a Nicolet Nic-Plan IR microscope used in a transmission mode. The spectrums were recorded within a range of 4000 to 650 $cm^{-1}$. The nominal resolution was 4 $cm^{-1}$. The Fourier transformation of 32 scans has been calculated using the Nicolet Omnic software version 7.1. Before each absorbance spectrum, a background spectrum was recorded.

### XRD

The XRD apparatus used was a Bruker AXS X-ray diffractometer equipped with a 2-D detector and a filtered Cu K$\alpha$ radiation source ($\lambda = 0.154059$ nm). The sample exposure time was 450 sec. The GADDS V 4.1.08 and Topas V 2.1 software were used for data analysis.

### Density properties

The densities of PUs were determined using the ASTM standard D-792.

### Thermal properties

A DSC Q100 from TA Instruments was used for the DSC measurements. This apparatus was equipped

with a refrigerated cooling system. All the measurements were performed under a nitrogen gas atmosphere. The DSC measurements were carried out following the ASTM standard procedure E1356-03. The thermal history was erased by heating the samples from 23°C to 100°C at a rate of 10°C/min after which the samples were cooled to −10°C at a rate of 5°C/min. The analysis was performed using the following procedure: performing a third cycle by heating from −10°C to 300°C at a heating rate of 10°C/min.

The Dynamic mechanical analyzer (DMA) used for this study was a DMA Q800 (TA instruments) equipped with a liquid nitrogen cooling system. The samples were analyzed following the ASTM standard E 1640. The sample dimensions for A-PU and S-PU were 17.3 mm × 7.7 mm × 1.4 mm and were analyzed in a single cantilever mode. The oscillation displacement and frequency were fixed at 0.015 mm and 1 Hz, respectively. The tests were performed over a temperature range of −100°C to 100°C. The multiple oscillation experiments were recorded as a function of frequency, ranging from 0.01 Hz to 100 Hz. These measurements were made every 5°C, over a temperature range of 30°C below and above the $T_g$ of the samples. The elastomeric plateau modulus built from the storage modulus master curves to find the average molecular weight between cross-links ($M_c$) and the concentration of elastically active network chains ($v_e$)using eq. (2)[25,26]:

$$G' = \frac{E'}{3} = aV_eRT = \frac{a\rho RT}{M_c} \quad (2)$$

Where $a$ has a value of 1 for the affine model and a value of $1 - \frac{2}{f}$ for the phantom model, with $f$ being the functionality.

### TGA-FTIR

The TGA instrument used was a Perkin Elmer Pyris 1. The purge gas used was nitrogen. The FTIR was a Thermo Nicolet Avatar 360 equipped with a 5 cm gas cell fitted with KBr windows. The cell was operated at room temperature. The FTIR spectra from 4000 to 400 wave numbers were obtained using Omnic software with 32 scans and 4 wave number resolution. The transfer line from the TGA to the FTIR gas cell was a 1 m length of 3 mm ID Tygon (PVC) tubing at ambient temperature. Before each absorbance spectrum, a background spectrum was recorded.

### Mechanical properties

The mechanical properties of the A-PU and S-PU samples were investigated using an Instron (MA) tensile testing machine (model 4202) equipped with a 50 KgF load cell and activated grips. Each sample was cut into four identical dumbbell shaped specimens and was cut using a V type cutter at a speed of 100 mm/min as suggested by the ASTM standard D638. Each sample was tested at room temperature.

## RESULTS AND DISCUSSION

### Separation of monomers

The separation of the monomers is shown in the HPLC chromatograph (Fig. 1). The asymmetric and symmetric monomers had a retention time of 7.4 min and 7.8 min, respectively. The difference in retention time was attributed to the asymmetric triol being less polar than the symmetric triol due to intramolecular hydrogen bonding between the two adjacent alcohol groups.[22]

### Characterization of polymers

The FTIR spectrum (Fig. 2) confirmed qualitatively the presence of the urethane linkage of both A-PU and S-PU. The characteristic N—H stretching vibrational region (3200–3500 $cm^{-1}$) and the characteristic C=O vibrational region (1700–1730 $cm^{-1}$) are well represented.[27] The bands in the region below 1600 $cm^{-1}$ represent the fingerprints of the PUs. The unreacted isocyanate (NCO group) is clearly shown by a peak centered at 2273 $cm^{-1}$.[25]

Figure 3 focuses on the C=O and N—H vibrational bands. The N—H stretching region showed two distinct bands. The band centered at 3444 $cm^{-1}$ corresponds to the free N—H region (3441–3446 $cm^{-1}$) and the band centered at 3329 $cm^{-1}$ corresponds to the bonded N—H region (3324–3329 $cm^{-1}$).[28,29] There are also two stretching regions attributed to the C=O group. The band centered at 1734 $cm^{-1}$ corresponds to the free carbonyl group

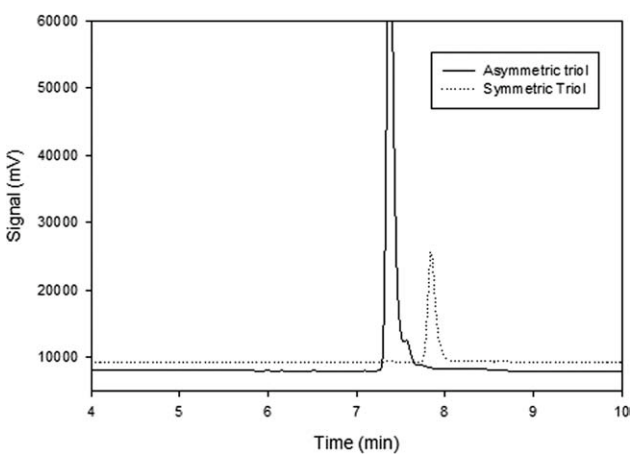


**Figure 1** HPLC retention times of the asymmetric and symmetric triol monomers.

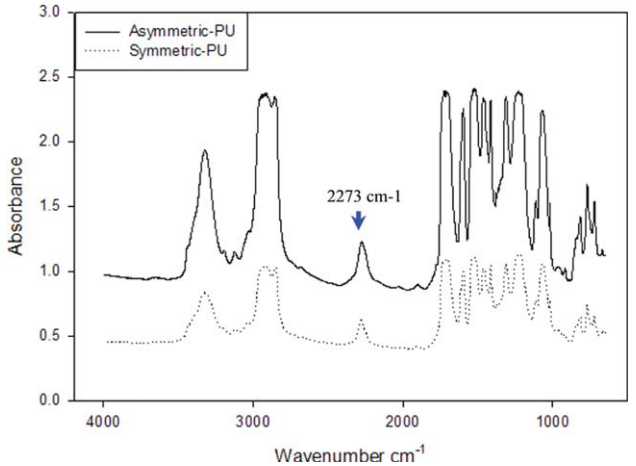


**Figure 2** FTIR spectra of A-PU and S-PU. [Color figure can be viewed in the online issue, which is available at www.interscience.wiley.com.]

(1731–1733 $cm^{-1}$) while the band centered at 1707 $cm^{-1}$ corresponds to the H-bonded-carbonyl group (1699–1706 $cm^{-1}$)[28,29] (Fig. 3). These results indicated that both of the PU matrices undergo physical bonding. The FTIR spectrum of the A-PU, S-PU, and M-PU[21] matrices were found to be similar.

The amorphous character of both the asymmetric and symmetric networks was verified by XRD (Fig. 4). The spectrum showed two broad peaks at $2\theta \approx 7^\circ$ and $2\theta \approx 20^\circ$. Similar results were found in other amorphous PUs.[30] The latter broad peak was identified as a characteristic of amorphous polymers.[21,31] The peak at $2\theta \approx 7^\circ$ is equivalent to an intermolecular distance of 1.7 nm. This long range ordering peak is usually found in segmented partially crystalline PUs. However, melting the sample to 300°C in the DSC (data not shown) did not reveal the presence of a high temperature melting peak, which further confirmed the amorphous structure of A-PU and S-PU.

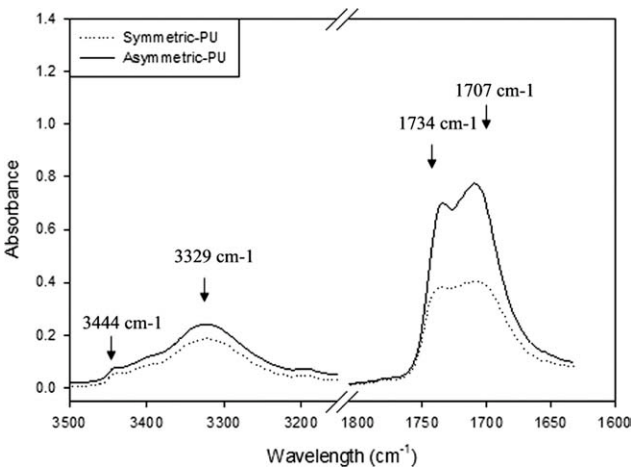


**Figure 3** FTIR spectra of C=O and N—H stretching of A-PU and S-PU.

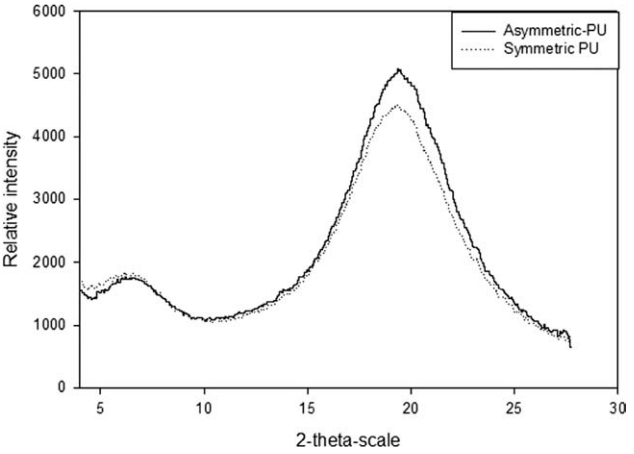


**Figure 4** WAXD data of A-PU and S-PU.

## Mechanical and physical properties

In this study, only the topological effect (crosslinking effect) could influence the $T_g$. $T_g$ values recorded by DSC were 24.2°C and 29.5°C for A-PU and S-PU, respectively (Table I). The differences in $T_g$ were explained by the concentration of unreacted isocyanate which could have been higher within the A-PU matrix than the S-PU matrix, suggesting that less MDI have reacted with the asymmetric monomers. This phenomenon could be explained by two factors. First, from the representation of the idealistic network structure (Fig. 5), the proximity of the alcohol groups in position 1 and 2 of the asymmetric structure could result in steric hindrance. Furthermore, the size of the MDI molecule might also played an important factor in reducing the interaction with the asymmetric monomer. When one MDI molecule reacts in position 1, a second molecule of MDI will have to overcome its steric hindrance before reacting in position 2.

Since the OH : NCO ratio used in the polymerization process of A-PU, S-PU, and M-PU was identical; the difference in $T_g$ was then explained by the difference in the post-curing conditions. In both cases, the gelation and the vitrification occurred at 75°C. Once the vitrification process is completed, the reactivity of the thermoset material decreases significantly. The post-curing at elevated temperature is then required to complete the reaction. The A-PU and S-PU post-curing conditions were 35°C lower than the

**TABLE I**
**Glass Transition Temperatures Obtained by DSC and DMA for the A-PU and S-PU Matrices**

| | $T_g$ (°C) from DSC | $T_g$ (°C) from DMA | ρ at 23°C ($g/cm^3$) |
|---|---|---|---|
| A-PU | 24.2 ± 0.4 | 34.8 ± 1.5 | 1.016 ± 0.006 |
| S-PU | 29.5 ± 0.8 | 40.4 ± 1.6 | 1.006 ± 0.002 |

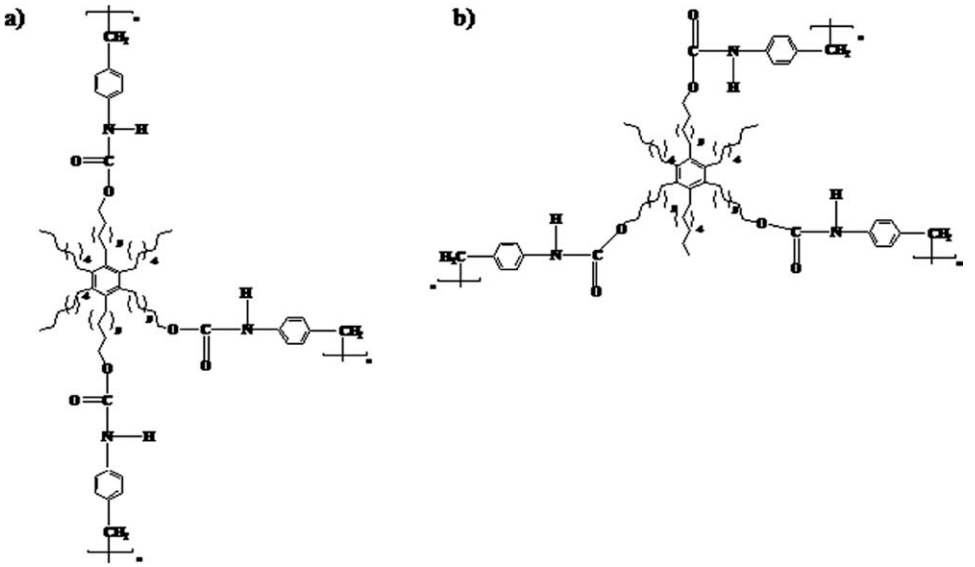


**Figure 5** Idealized network structures.

M-PU (110°C). Monteavaro et al.,[32] who worked with PU networks from soy oil, reported a $T_g$ variation of 5°C when applying a variation of 40°C in the post-curing process. However, Li and Larock[33] reported that the crosslinking density of their soybean oil PUs decreased when post-cured at 110°C for an exposure time of 5 h. Consequently, since the curing behavior of the A-PU, S-PU, and M-PU are not well understood due to their novelty, the post-curing condition of the A-PU and S-PU was set at 75°C to avoid the decrosslinking.

A higher $T_g$ value is an indication of the increase in chain connectivity. It raises the stiffness of the matrix and thus reduces the loss modulus. This was observable by the tan curves (Fig. 6), where the ratio of the loss modulus to the storage modulus is shown. The PU samples experienced a general trend, where the tan δ peak intensity decreased as the crosslinking density increased. Figure 6 also revealed that the A-PU and S-PU have similar damping properties that corresponded to a tan δ value $\geq$0.3 over a range of temperature greater than 20°C. These specifications fulfilled the requirements for efficient damping properties of homopolymers.[34] The curves maxima also corresponded to the transition from the glassy state to the rubbery state. The corresponding temperature is also reported as the $T_g$ (Table I).

The $T_g$ values of both polymers being close to room temperature, the stress-strain curves of the samples showed a behavior similar to rubber (Fig. 7). The trend in the modulus of both PUs at low strain was found to be different. It is suggested that a higher crosslinking density of the S-PU would have raised the modulus, which would be in agreement with the $T_g$ values and the DMA results. A-PU

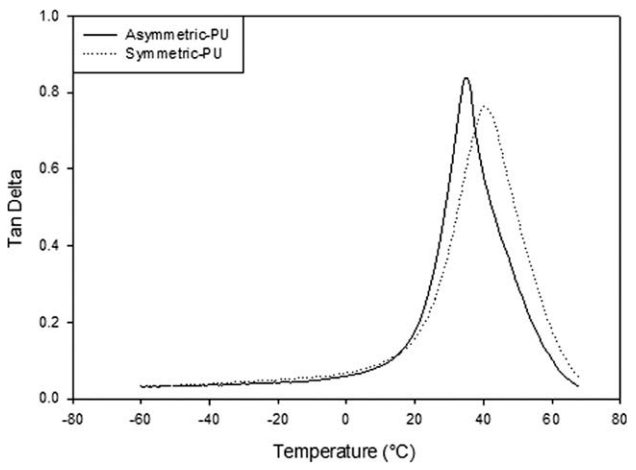


**Figure 6** Loss tangent of A-PU and S-PU measured by DMA.

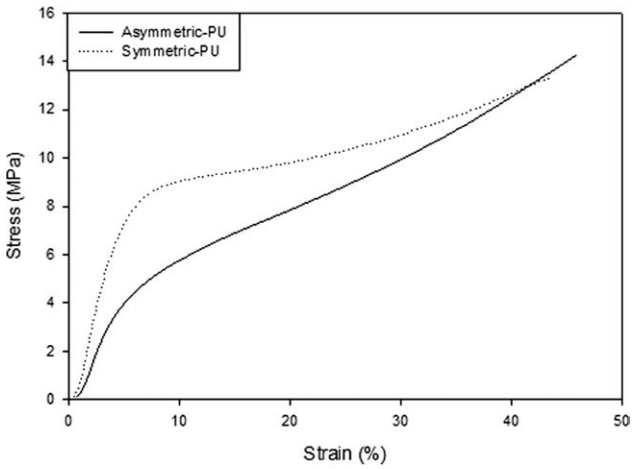


**Figure 7** Stress-strain curve of A-PU and S-PU.

displayed a tensile stress and an elongation at break of 13 MPa ± 1% and 46 ± 3%, respectively. S-PU displayed a tensile stress and an elongation at break of 14 MPa ± 1% and 50 ± 9%, respectively. The similarity of these results can be explained by the fact that both matrices had the same ratio of aromatic content, the same carbon-carbon chain length between the aromatic structure and the hydroxyl groups, and the same ratio of dangling chains. It is then expected that the M-PU would have the same mechanical properties as the A-PU and S-PU. Vegetable oil based PUs crosslinked with MDI having similar OH : NCO ratio and functionality as the A-PU and S-PU provide a wide range of mechanical properties. As a comparison, the tensile strengths of A-PU and S-PU were of lower values but higher elongation at break than of epoxidized soybean oil PUs (46 MPa, 7%),[35] and rhodium catalyzed hydroformylated soybean oil-PU (38 MPa, 17%).[4] Inversely, the A-PU and S-PU had similar tensile strength and lower elongation at break than ozonolyzed-hydrogenated canola oil based PU (14 MPa, 75%).[25]

An attempt to evaluate the $M_c$ and $v_e$ values through the elastomeric plateau modulus built from the storage modulus master curves was made using eq. (2). The rubber elasticity theory proposes the affine and phantom models, among others, for the evaluation of $M_c$ and $v_e$. The affine network model assumes that (1) the network deformation is proportional to the deformation of the network strands and (2) that the junction points are pinned to an elastic background and do not fluctuate during deformation.[36] The later assumption is also valid for the phantom model but only at the chains' end. It also acknowledges that the crosslinks can fluctuate around their average position. However, the model assumes the strands to be ideal, i.e., the chain ends to be joined at crosslinks. As a consequence, this model neglects the defects that normally occur in a real network such as dangling ends and dangling loops. Since the phantom model allows the strands to unrestrictedly fluctuate, it lowers the modulus value if compared to the affine model, where the junctions are considered steady. A real network will then have a modulus value lower than the one predicted by the affine model but higher than the one predicted by the phantom model.

In this study, $T_g$ values from the tan δ plot were used as the reference temperatures for the construction of the storage modulus ($E'$) master curve as a function of the log of the reduced frequency ($fa_t$). The viscoelastic responses of the A-PU and S-PU were then acquired based on the time-temperature superposition principle by shifting the isothermal response curves along the horizontal axis, with the exception of the responses at reference temperature (Fig. 8). No vertical shift was applied.

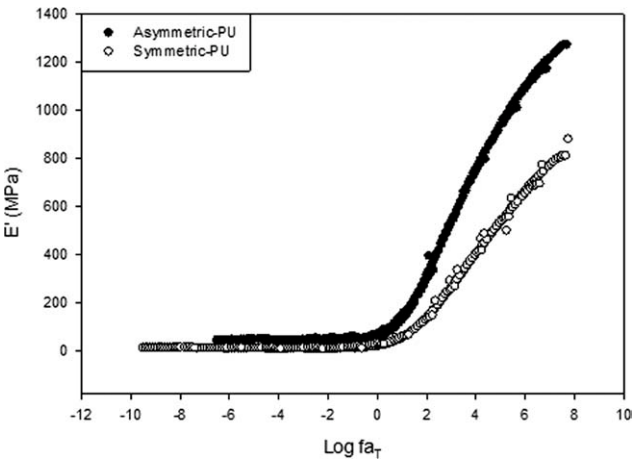


**Figure 8** Master curves of $E'$ for A-PU and S-PU.

As the $T_g$ value of the S-PU matrix was higher in both DMA and DSC results and due to the trend of the tan δ curves explained previously (Fig. 6), it was expected that the plateau modulus of the A-PU matrix would have a lower $E'$ value than the S-PU matrix. Surprisingly, the $E'$ values at the plateau were 44 MPa and 12 MPa for A-PU and S-PU, respectively. Consequently, the corresponding $M_c$ values were 177 g/mol (A-PU) and 654 g/mol (S-PU). Clearly, this method has been unsuccessful regarding the present samples since these $M_c$ values correspond to a point of crosslink at every 14 (A-PU) and 54 (S-PU) carbons. It is worth mentioning that Lligadas et al.[21] also made an attempt to make a qualitative evaluation of the crosslinking density through the DMTA technique. It was found that the $E'$ plateau value of more tightly crosslinked matrices was lower than less crosslinked matrices, which is also a deviation from the normal trend.

## Thermal stability

The TGA-FTIR was used to study the thermodegradation patterns of the monomers and polymers. The asymmetric monomers presented one degradation phase of 2.18%/°C at 442°C and the symmetric monomers presented one phase of 1.88%/°C at 433°C (data not shown). These degradation stages were studied through FTIR under an inert gas and showed a characteristic band at 2920 $cm^{-1}$, which revealed the release of octene attributed to the degradation of the monomer's dangling chains. Because the release of octene was first noted at approximately 365°C for both monomers, it was assumed that their thermostability was similar.

The thermodegradation stages of vegetable oil based polyurethane networks have been commonly studied through TGA. From the TGA curves (Fig. 9), a 5% weight loss was present at 321°C (A-PU) and 314°C (S-PU). These temperatures are comparable to

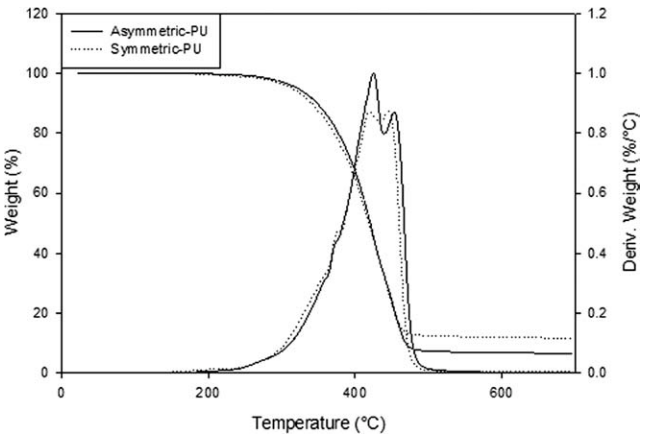


**Figure 9** Thermal stability and first derivative curves of A-PU and S-PU in function of the temperature.

the M-PUs which presented a 5% weight loss at 327°C. Interestingly, the A-PU and S-PU were found to be thermally more stable than the aromatic triol based PUs from cardanol.[23] This latter did exhibit a 10% weight loss at 250°C compared to roughly 340°C for the A-PU and S-PU.

Javni et al.,[7] who worked with eight types of vegetable oil based PUs of functionality varying from 2 to 4, demonstrated that these PUs shows two to three degradation phases. The first derivative curves of the A-PU and S-PU showed that their thermodegradation patterns were similar. The A-PU presented two degradation phases: 1.00%/°C at 424°C and 0.87%/°C at 454°C. The symmetric-PU also presented two phases: 0.87%/°C at 421°C and 0.87%/°C at 446°C. The first volatile compound detected for both samples showed characteristic bands at 2354 $cm^{-1}$ and 667 $cm^{-1}$, indicating a release of $CO_2$. It is known that vegetable oil based PUs start their degradation by dissociation into polyols and precursors of urethanes.[7] The release of $CO_2$ gas was associated to the dissociation of urethane linkage into primary amine and olefin.[37] Similarly to their corresponding monomers, the degradation of the dangling chains started at 365°C for both matrices. The FTIR detected the presence of octene at the last degradation step for both samples. Finally, the ring degradation started at 700°C, indicated by the presence of carbon monoxide at 2150 $cm^{-1}$ and either ethylene or ethene at 959 $cm^{-1}$ for both matrices.

## CONCLUSIONS

This study was conducted to determine the effect of the hydroxyl group positioning of the asymmetric and symmetric monomers on the different mechanical and physical properties of their corresponding PUs matrices. It was qualitatively determined by FTIR that both of the PU matrices had unreacted isocyanate. It was also determined that the urethane linkage was existent for both matrices. The $T_g$ of A-PU was lower than the S-PU. It was assumed that less crosslinker reacted with the asymmetric monomers probably due to the steric hindrance induced by the two adjacent hydroxyl groups. However, both of these matrices had similar stress and strain at break. It also was found that the geometry of the monomers and their corresponding PU matrices did not have a significant impact on the thermodegradation of the matrices.

The authors thank Mr. Ereddad Kharraz for his technical expertise and Dr. Carla Spina for editing.

## References

1. Petrovic, Z. S. Polym Rev 2008, 48, 109.
2. Abraham, T. W.; Carter, J. A.; Malsam, J.; Zlatanic, A. B. (to Pittsburg State University, USA). U.S. Pat. 2006–786,594 (2007); p 47.
3. Guo, A.; Cho, Y. J.; Petrovic, Z. S. J Polym Sci A Polym Chem 2000, 38, 3900.
4. Guo, A.; Demydov, D.; Zhang, W.; Petrovic, Z. S. J Polym Environ 2002, 10, 49.
5. Guo, A.; Zhang, W.; Petrovic, Z. S. J Mater Sci 2006, 41, 4914.
6. Hu, Y. H.; Gao, Y.; Wang, D. N.; Hu, C. P.; Zu, S.; Vanoverloop, L.; Randall, D. J Appl Polym Sci 2002, 84, 591.
7. Javni, I.; Petrovic, Z. S.; Guo, A.; Fuller, R. J Appl Polym Sci 2000, 77, 1723.
8. Kaushik, A.; Singh, P. Int J Polym Anal Charact 2005, 10, 373.
9. Lysenko, Z.; Schrock, A. K.; Babb, D. A.; Sanders, A.; Tsavalas, J.; Jouett, R.; Chambers, L.; Keillor, C.; Gilchrist, J. H. (to Dow Global Technologies, Inc., USA). U.S. Pat. 2004-12,427 (2004); p 68.
10. Narine, S. S.; Yue, J.; Kong, X. H. J Am Oil Chem Soc 2007, 84, 173.
11. Petrovic, Z.; Guo, A.; Javni, I. (to Pittsburg State University, USA). U.S. Pat. 98–187,992 (2000); p 8.
12. Petrovic, Z. S.; Guo, A.; Zhang, W. J Polym Sci A Polym Chem 2000, 38, 4062.
13. Shah, A.; Shah, T. (;to Polymermann (Asia) Pvt. Ltd., India). U.S. Pat. 2000-18,895 (2001); p 10.
14. Tran, P.; Graiver, D.; Narayan, R. J Am Oil Chem Soc 2005, 82, 653.
15. Tu, Y. C.; Suppes, G. J.; Hsieh, F. H. J Appl Polym Sci 2008, 109, 537.
16. Tu, Y. C.; Suppes, G. J.; Hsieh, F. H. J Appl Polym Sci 2009, 111, 1311.
17. Yue, J.; Narine, S.; Sporns, P. Can. Pat. 2006–2531977 (2007). p 121.
18. Zlatanic, A.; Lava, C.; Zhang, W.; Petrovic, Z. S. J Polym Sci B Polym Phys 2004, 42, 809.
19. Zlatanic, A.; Petrovic, Z. S.; Dusek, K. Biomacromolecules 2002, 3, 1048.
20. Petrovic, Z. S.; Zhang, W.; Javni, I. Biomacromolecules 2005, 6, 713.
21. Lligadas, G.; Ronda, J. C.; Galia, M.; Cadiz, V. Biomacromolecules 2007, 8, 1858.
22. Yue, J.; Narine, S. S. Chem Phys Lipids 2008, 152, 1.
23. Suresh, K. I.; Kishanprasad, V. S. Ind Eng Chem Res 2005, 44, 4504.
24. Song, D.; Narine, S. S. Chem Phys Lipids 2008, 155, 43.
25. Kong, X.; Narine, S. S. Biomacromolecules 2007, 8, 2203.
26. Kong, X. H.; Yue, J.; Narine, S. S. Biomacromolecules 2007, 8, 3584.

27. Wang, F. C.; Feve, M.; Lam, T. M.; Pascault, J. P. J Polym Sci B Polym Phys 1994, 32, 1305.
28. Tsai, Y. M.; Yu, T. L.; Tseng, Y. H. Polym Int 1998, 47, 445.
29. Goddard, R. J.; Cooper, S. L. Macromolecules 1995, 28, 1390.
30. Petrovic, Z. S.; Fajnik, D. J Appl Polym Sci 1984, 29, 1031.
31. Lligadas, G.; Ronda, J. C.; Galia, M.; Cadiz, V. Biomacromolecules 2006, 7, 2420.
32. Monteavaro, L. L.; Da Silva, E. O.; Costa, A. P. O.; Samios, D.; Gerbase, A. E.; Petzhold, C. L. J Am Oil Chem Soc 2005, 82, 365.
33. Li, F. K.; Larock, R. C. Polym Int 2003, 52, 126.
34. Li, F. K.; Larock, R. C. Polym Adv Technol 2002, 13, 436.
35. Petrovic, Z. S.; Zhang, W.; Zlatanic, A.; Lava, C. C.; Ilavsky, M. J Polym Environ 2002, 10, 5.
36. Rubinstein, M. Polymer Physics; Oxford University Press: New York, 2003.
37. Ketata, N.; Sanglar, C.; Waton, H.; Alamercery, S.; Delolme, F.; Raffin, G.; Grenier-Loustalot, M. E. Polym Polym Compos 2005, 13, 1.